American Journal of Pathology, Vol. 145, No. 4, October 1994

Lymphoproliferative Disease in Mice Infected with Murine Gammaherpesvirus 68

N. P. Sunil-Chandra, J. Arno, J. Fazakerley, and A. A. Nash

From the Department of Pathology, University of Cambridge, Cambridge, United Kingdom

Murine gammaherpesvirus is a natural pathogen of wild rodents. In the laboratory it establishes an infection of epithelial cells and persists in B lymphocytes in a latent form. Inbred mice chronically infected with the virus develop a lymphoproliferative disease (LPD) similar to that seen in patients infected with Epstein-Barr virus. The frequency of LPD over a period of 3 years was 9% of all infected animals, with 50% of these displaying high grade lymphomas. The incidence of LPD was greatly increased when infected mice were treated with cyclosporin A. The majority of mice used in the experiments were BALB/c, although lymphomas were detected in mice on other genetic backgrounds, ie, CBA and B10Br. Lymphomas were associated with both lymphoid and nonlymphoid tissues (liver, lung, and kidney). In all cases of lymphomas studied thus far, there was a mixed B cell (B220+ve) and T cell (CD3+ve) phenotype. The B cells were light chain restricted, indicative of a clonal origin. Variable numbers of virus genome-positive cells were detected by in situ hybridization in and around the lymphomas. In contrast, no lytic antigen-positive cells were detected, indicating that genome-positive cells were either latently infected or undergoing an abortive infection. These observations suggest that murine gammaherpesvirus-infected mice may be an important model to study the pathogenesis of LPD associated with other gammaherpesviruses, such as Epstein-Barr virus. (Am J Pathol 1994, 145:818–826)

The gammaherpesviruses are divided into two subgroups: gamma 1 viruses represented by Epstein-Barr virus (EBV) and gamma 2 viruses typified by herpesvirus saimiri (HVS) and other related viruses of New World monkeys. These viruses are associated with lymphoproliferative disease (LPD) in the infected host and can efficiently transform lymphocytes infected *in vitro*. EBV, the causative agent of infectious mononucleosis, is also associated with Burkitt's lymphoma, nasopharyngeal carcinoma, and a variety of LPDs observed in immunocompromised individuals such as those with AIDS and in posttransplant patients.[1,2] In contrast, HVS causes an inapparent infection in the natural host but induces polyclonal lymphoid neoplasia in related species.[3]

Animal models have contributed greatly to our understanding of alphaherpesvirus and betaherpesvirus infections. Models of EBV infection have proven to be more difficult to establish, although some forms of LPD have been induced in primates and severe combined immunodeficiency (SCID) mice.[1–7] More recently, a mouse gammaherpesvirus has been described that is a natural pathogen of wild rodents, ie, voles and mice.[8,9] Infection of laboratory mice with this virus results in replication in alveolar epithelial cells and the establishment of a persistent/latent infection in B lymphocytes.[10,11] Furthermore, this virus will also infect myeloma cells (B cell lineage) *in vitro*, where a state of latency can be produced in which the viral genome exists in an episomal form.[12]

In mice chronically infected with MHV-68, we have identified a variety of pathological changes with a high incidence of LPD. The latter showed a range of histological appearances and affected both lymph nodes and spleen, as well as extranodal sites. In the case of lymphomas the magnitude of the disease ranged from low grade to high grade lymphomas, associated with both lymphoid and nonlymphoid tissue. In this report we describe our findings on the nature of the tumors produced and the association of these with the virus.

Supported by a grant from the Medical Research Council of Great Britain.

Accepted for publication June 27, 1994.

Address reprint requests to Professor Anthony A. Nash, Department of Veterinary Pathology, University of Edinburgh, Summerhall, Edinburgh EH9 1QH, UK.

Materials and Methods

Mice

Female BALB/c (H-2^d), C57BL/10 (H-2^b), and CBA (H-2^k) mice were obtained from Bantin and Kingman (Hull, UK) or Olac Ltd. (Bichester, UK) and were infected at 3 to 4 weeks of age. Animals were maintained in three different animal units during the course of these experiments. Mouse hepatitis virus and Sendai virus were identified in two of the units.

Virus

MHV-68 was originally obtained from Professor D. Blaskovic[8] and the clone G2.4 was isolated.[9,13] Virus was grown in BHK cells at a low multiplicity of infection (0.1 pfu/cell) and working stocks stored at −70 C.[10]

Intranasal and Intravenous Infection of Mice

Mice were inoculated intranasally or intravenously with 4×10^5 pfu of MHV-68. Approximately 40 μl of virus was administered intranasally to mice under light anesthesia. For intravenous inoculation, 0.1 ml of the virus dilution was injected into the tail vein. Mice were caged in groups of four. No evidence of horizontal transmission of this virus has so far been detected between groups of infected and uninfected mice (unpublished observations).

Cyclosporin A (CsA) Treatment of MHV-68-Infected Mice

A group of infected animals were treated with CsA (a gift from Dr. D. White, Department of Surgery, Addenbrookes Hospital, Cambridge, UK). Infected mice were injected intraperitoneally with 1 mg CsA in 0.1 ml of olive oil (equivalent to 50 mg/kg) on 3, 7, 14, 21, and 28 days after the first injection. Another group of infected animals received olive oil only.

Histopathological and Immunohistochemical Studies

Various tissues (heart, kidney, lung, liver, spleen, thymus, mesenteric lymph nodes, pancreas, uterus, ovary, and adrenal gland) were removed from mice with clinical evidence of lymphomas and latently infected mice with no clinical signs of disease at various times after infection and immediately fixed in 10% buffered formal saline. Organs from uninfected mice acted as negative controls. Tissues were paraffin embedded and 5-μ-thick sections were stained with hematoxylin and eosin (H&E). In some experiments tissues were removed then snap-frozen and prepared for cryostat sections. Indirect immunoperoxidase antibody labeling was used to detect virus antigen, CD3 (rat IgG2a, clone KT3; a gift from Dr. K. Tominari, Clinical Research Centre, Harrow, UK) and B220 (rat IgG2a, clone R36B2; Pharmingen, San Diego, CA), as described by Sunil-Chandra et al.[10] Briefly, paraffin processed tissue sections were treated with 0.1% trypsin for 5 minutes to avoid problems associated with overfixation of tissue specimens in formalin. Nonspecific binding of antibodies was minimized by the use of Tris-buffered saline for diluents and rinsing and by addition of a blocking step, which included 5% normal goat serum and 10% bovine serum albumin in the case of viral antigen or 5% normal rabbit serum in the case of CD3 or B220 surface antigens. Endogenous peroxidase activity was minimized by immersing the slides in a solution of 0.75% hydrogen peroxide in methanol for paraffin sections or 0.3% hydrogen peroxide diluted in Tris-buffered saline for cryostat sections for 30 minutes. After this period all paraffin sections were trypsin treated for 5 minutes. Immunoperoxidase staining with an avidin/biotin detection system using either goat anti-rabbit IgG [heavy and light] chain biotinylated antibody for viral antigens or rabbit anti-rat IgG [heavy and light] chain biotinylated antibody for mouse surface antigens) was performed using the Vectastain ABC kit (Vector Laboratories, Bretton, Peterborough, UK).

Direct immunoperoxidase antibody labeling was used to detect κ- and λ-chains using clonotyping system II kit (SeraLab, Crawley Down, Sussex, UK). This included goat anti-mouse κ and λ antibodies labeled with horseradish peroxidase. DAB was used as the substrate for direct and indirect immunostaining.

In Situ *Hybridization*

Tissue sections were prepared for *in situ* hybridization, as described previously.[10] Briefly, this involved treating tissue sections with proteinase K, followed by prehybridization (1 hour at 37 C) and then hybridization with a 1.2-kb DNA probe (boiled for 5 minutes and rapidly chilled on ice before adding to the hybridization solution). To achieve a higher sensitivity, the 1.2-kb terminal repeat fragment of MHV-68 genome[9,13] was used for preparation of ^{35}S-labeled DNA probes by random hexanucleotide priming. The

pUC13 plasmid DNA-negative control probe and tissue sections obtained from spleen, kidney, liver, lung, heart, and mesenteric lymph node of an uninfected mouse were also included to confirm the specificity of hybridization. Immediately after addition of probe the tissue sections were heated to 80 C for 10 minutes. Hybridization was for 18 hours at 37 C. Sections were then washed twice for 15 minutes with 2× standard saline citrate (SSC) at room temperature, twice for 15 minutes with 0.1× SSC at room temperature, and once for 10 minutes with 0.1× SSC preheated to 60 C and kept at 37 C followed by a 15-minute wash with 2× SSC at 60 C. The sections were then dehydrated via a series of graded alcohols, air-dried dipped in photographic emulsion (prepared in a dark room by adding 20 ml of Amersham LM-1 emulsion to 20 ml of 0.66 M ammonium acetate at 42 C), allowed to dry at room temperature in a light-tight box for 2 hours, and autoradiographed for 1 to 4 weeks at 4 C. Slides were developed, fixed, counterstained with H&E, dehydrated, and mounted in DePeX.

Results

Pathological Changes in Mice Latently Infected with MHV-68

The long-term pathological effects of MHV-68 infection were studied in 220 mice obtained from three different animal units (see Materials and Methods). These included 18 BALB/c mice infected intravenously and 162 BALB/c, 20 C57BL/10, 10 B10Br, and 10 CBA mice infected intranasally. The animals were examined for the development of any clinical features over a period of 3 years after recovery from the primary infection. Twenty-five of 220 (11%) mice became clinically sick starting at varying times from 165 to 825 days postinfection (Table 1). These mice and a group of clinically normal mice (15 of 220) were killed during this postinfection period and various tissues examined for gross pathological and histopathological changes. In more than 300 uninfected BALB/c mice monitored under similar animal housing conditions for similar time periods, no evidence of clinical LPD or lymphomas were observed.

Clinical and Gross Pathological Features

Sick mice showed either moderate to massive enlargement of the abdomen with abnormal gait or weakness and emaciation. Animals with distended abdomens usually had nodular splenomegaly, nodular hepatomegaly, or enlarged kidneys and in addition some animals had lymphoid tumors of the mesenteric lymph nodes, pancreas, ovary, or intestine (Figure 1). In some animals, however, the abdominal distension was caused by massive hemorrhagic uterine cysts.

Table 1. *Pathological Features of MHV-68-Infected Mice During a Long-Term Latent Infection*

Mouse	Days PI	Strain/Route*	Histopathological Features
1	165	BALB/c, i.n.	Mild LPD in lung and CBP
2†	170	BALB/c, i.n.	Mild LPD in lung and MLN
3	286	BALB/c, i.n.	Mild LPD in lung and AT
4	290	BALB/c, i.n.	AT and HEP in S
5	350	C57Bl, i.n.	Adenocarcinoma in the lung
6	376	BALB/c, i.n.	Mild LPD in lung, K, CBP, and HEP in L
7	400	BALB/c, i.n.	Uterine cyst
8	540	BALB/c, i.n.	Mild LPD in K and carcinoma in O
9	540	BALB/c, i.v.	HGL in SP, L, K, lung, and MLN
10	635	B10Br, i.n.	Focal nodular hyperplasia in L
11	665	CBA, i.n.	Sarcoma of muscle
12	715	BALB/c, i.n.	HGL in S, K, MLN, L, lung, and MGC
13	725	BALB/c, i.n.	Mild LPD in K, L, lung, AT, and uterine cyst
14	725	C57Bl, i.n.	Mild LPD in lung, A, and HEP in L
15	725	BALB/c, i.n.	HGL in MLN and P
16	725	BALB/c, i.n.	HGL in S, K, L, and lung
17	725	C57Bl, i.n.	HGL in MLN and S
18	740	BALB/c, i.n.	Mild LPD in K, lung, and INT
19	740	BALB/c, i.n.	Mild LPD in lung, tumor in O
20	767	BALB/c, i.n.	Nodular LGL in S, lung, L, and K
21	790	BALB/c, i.n.	Mild LPD in lung, L, K, AT, and HEP in S
22	810	C57Bl, i.n.	HGL in S, L, MLN, O, K, A, and lung
23	810	CBA, i.n.	HGL in S and L
24	824	BALB/c, i.n.	LGL in K, lung, L, and uterine cyst
25	824	BALB/c, i.n.	Mild LPD in lung, CBP, and uterine cyst
26	834	BALB/c, i.n.	MGC

PI, postinfection; i.n., intranasal infection; i.v., intravenous administration; HGL, high grade lymphoma; LGL, low grade lymphoma; LPD, lymphoproliferative disease; CBP, chronic bronchopneumonia; HEP, hemopoiesis; AT, atrial thrombosis; MGC, mammary gland carcinoma; S, spleen, K, Kidney; MLN, mesenteric lymph node; L, liver; A, adrenal gland; O, ovary; P, pancreas; INT, intestine.

* Mice were infected with 4×10^5 pfu virus except no. 7 which received 2×10^4 pfu.

† All mice except no. 2 were clinically sick.

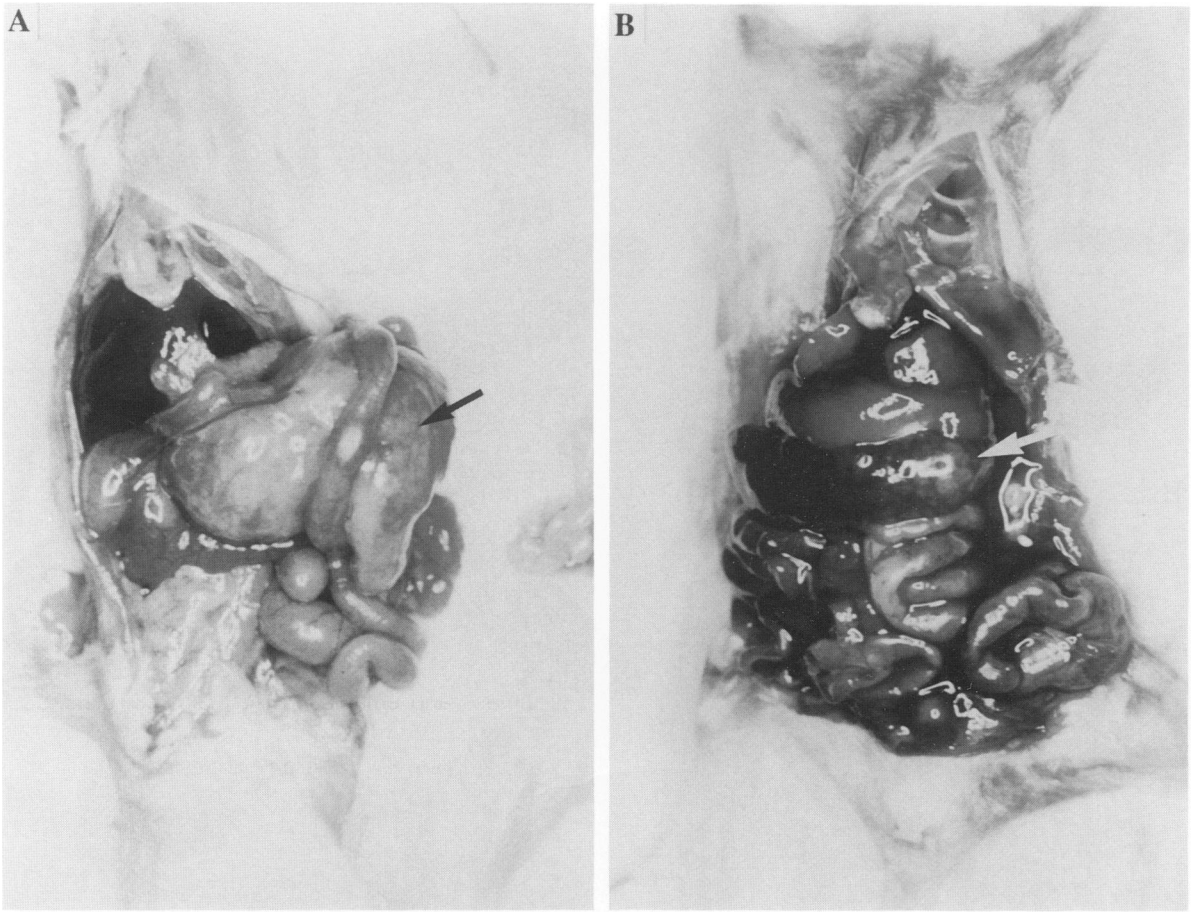

Figure 1. *Gross pathological features of lymphomas detected in BALB/c mice infected with murine gammaherpesvirus.* **A:** *An intra-abdominal lymphoma within the mesentery of mouse no. 15 at 725 days postinfection (indicated by an arrow).* **B:** *Splenomegaly in mouse no. 16 (at 725 days postinfection) as a result of extensive splenic involvement by abnormal lymphoid cell masses that appear as yellowish-white nodular areas (indicated by an arrow).*

Animals with weakness and emaciation had consolidation of the lung or enlarged hearts with lesions in the atrium (Table 1).

Histopathological Changes

Among the 25 sick mice, 20 (9% of total) had developed lymphoproliferative disorders. In nine of these, the disease was judged to be high grade lymphoma most resembling centroblastic/centrocytic or plasmablastic non-Hodgkin's lymphomas seen in humans. There was cellular pleomorphism and a high mitotic rate. In some animals, abnormal plasma cells and occasional cells resembling Reed-Sternberg cells in appearance were observed in the spleen (data not shown). Spleen, mesenteric lymph nodes, liver, lung, and kidney were the organs mainly affected (Figure 2, A-C). In the spleen the normal lymphoid tissue was replaced by nodular masses of lymphoma. In the lung, lymphomatous tissue was distributed around both bronchi and blood vessels; in the liver primarily within portal tracts and in the kidney, deposits were particularly peripelvic or subcapsular (Figures 2 and 4). In some cases, replacement of tissue parenchyma was extensive.

When the histological appearance was that of a milder lymphoproliferative disorder, a similar distribution to that described above was found, the lesions being most obvious in lung, liver, and kidney. It may be postulated that the lesser lymphoproliferative state might constitute the basis from which the high grade lymphomas would arise.

In 1 of 15 (mouse no. 2) latently infected but apparently normal mice that were examined, there was mesenteric node enlargement and consolidation of the lungs characterized by histological appearance of mild LPD.

Not all the clinically sick mice had LPD. Four had a form of bronchopneumonia and six had lesions in the heart. The former had purulent exudate within bronchi that were surrounded by dense plasma cell infiltration. Sometimes it was believed that mild LPD

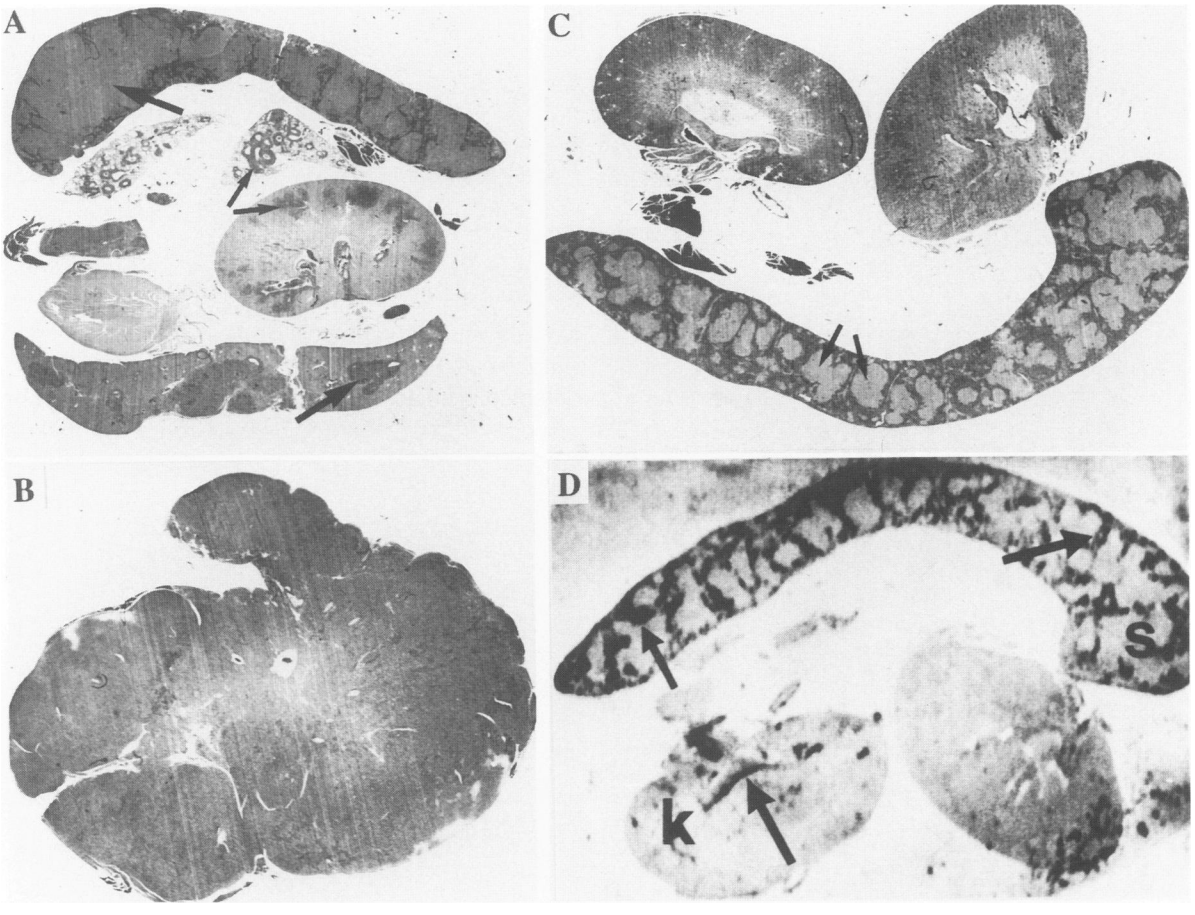

Figure 2. *Anatomical distribution of lymphomas in various organs of affected mice.* A: *H & E-stained tissue sections of spleen, lung, kidney, and liver of mouse no. 16 shown in* (B) *that are infiltrated histologically by a high grade lymphoma* (*indicated by arrows*) (*magnification* ×4). B: *H & E-stained section of the mesenteric lymph node shown in* (A) *of mouse no. 15* (*magnification* ×4). C: *H & E-stained sections of spleen and kidneys of mouse no. 9. Arrows indicate massive lymphoid cell masses that occupy extensive areas of the spleen* (*magnification* ×4). D: *Autoradiographic film images of an adjacent tissue section taken from spleen and kidney shown in* (C) *of mouse no. 9 hybridized with a* ^{35}*S-labeled MHV-68 DNA* (*1.2-kb terminal repeat fragment*) *probe* (*magnification* ×4). In situ *hybridization shows the distribution of viral DNA in the spleen surrounding lymphoid masses* (*indicated by arrows*). *In the kidney signal is preferentially localized to central collecting area.* In situ *hybridization using negative control* ^{35}*S-labeled probe* (*pUC 13 plasmid DNA*) *in the adjacent sections showed no positivity* (*data not shown*).

might also be present but it was impossible to be certain against the background of severe chronic inflammation. The abnormality affecting the heart in some cases was thrombosis in a dilated atrium, a finding that would argue for some cardiac dysrhythmia before death. Six of 220 mice showed evidence of increase in extramedullary hemopoiesis, suggesting that there was bone marrow impairment (Table 1). Furthermore, 6 of 220 animals had uterine abnormalities. These consisted of endometrial hyperplasia and cystic enlargement of the uterus filled by blood-stained fluid. The occurrence of other pathological lesions such as mammary gland carcinoma (2 of 220), adenocarcinoma of the lung (1 of 220), focal nodular hepatic hyperplasia (1 of 220), and a sarcoma arising in skeletal muscle (1 of 220) were also observed.

Phenotype and Clonality of Lymphomas

A group of 30 MHV-68-infected mice were treated with CsA, as described in Materials and Methods. The CsA-treated and untreated group of animals were then monitored for the development of clinical signs. Over a period of 12 months, 60% of CsA-treated and 20% of untreated mice developed LPD affecting both lymphoid and nonlymphoid tissue. A series of lymphoid tumors from the infected mice were analyzed for the membrane phenotype of lymphocytes by immunoperoxidase staining of cryostat sections. Of seven mice investigated with high grade lymphomas, all showed a mixed T (CD3 positive) and B (B220 positive) cell phenotype, with CD4 T cells as the major T cell subset. In all cases, the B cells showed light

chain restriction: five with κ-chain and two with λ-chain (Figure 3). In two cases the light chain restriction was associated with plasma cells. This suggests a clonal derivation of B cells in these tumor-bearing animals.

Detection and Distribution of Viral DNA-Positive Cells in Organs Affected with Lymphomas

In situ hybridization was used to detect viral DNA on tissue sections of the mice presented in Table 1. An increased number of positive cells were observed in organs with mild LPD or high grade lymphomas when compared with spleen sections from latently infected normal mice[10] or mice with other pathological (non-LPD) conditions.

Mouse no. 9 developed a massively enlarged abdomen at 540 days postinfection. Pathological examination demonstrated dramatic nodular hepatosplenomegaly and enlarged kidneys and mesenteric lymph nodes as a result of lymphoma. Initially, *in situ* hybridization was performed on tissue sections with and without heating to 80° C to detect viral DNA and RNA, respectively. Hybridization signal was apparent in the spleen and kidney only in the treated sections, suggesting that DNA is present in these cells but RNA transcripts were absent or below the level of detection (Figure 2, D).

In situ hybridization on several sections of spleen and kidney obtained from mouse no. 9 repeatedly showed virus genome-positive cells associated with lymphomas (Figure 4, a and d). No virus antigen was detected in adjacent sections of these organs by immunoperoxidase labeling (Figure 4, b and e). In the same experiment, virus antigen could be detected in lung tissue obtained from an acutely infected animal. This observation strongly suggests that the positive signal observed in association with the lymphoma is due either to the presence of latent virus or an abortive virus infection.

Studies on the tissues taken from other affected animals showed DNA-positive cells in all the lympho-

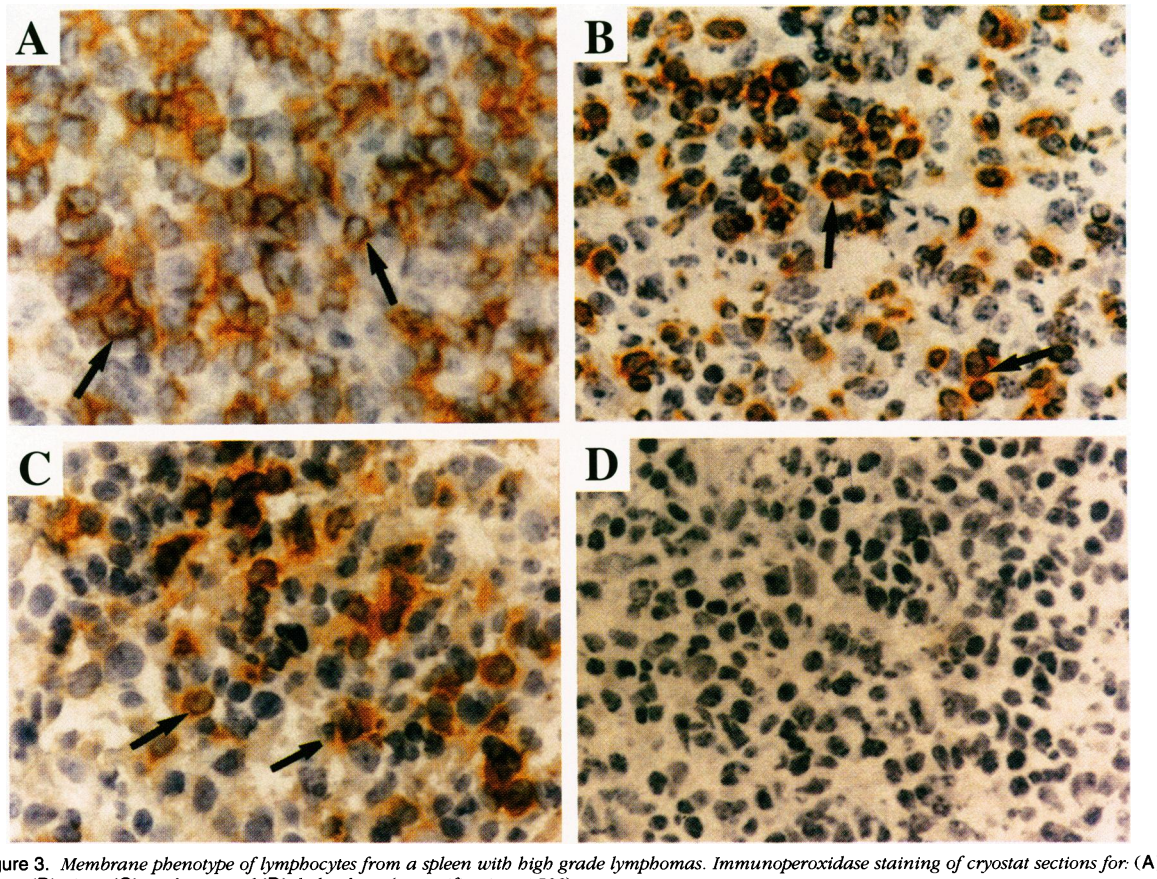

Figure 3. *Membrane phenotype of lymphocytes from a spleen with high grade lymphomas. Immunoperoxidase staining of cryostat sections for:* (A) *B220,* (B) *CD3,* (C) *κ-chain, and* (D) *light chain* (*magnification* × 500).

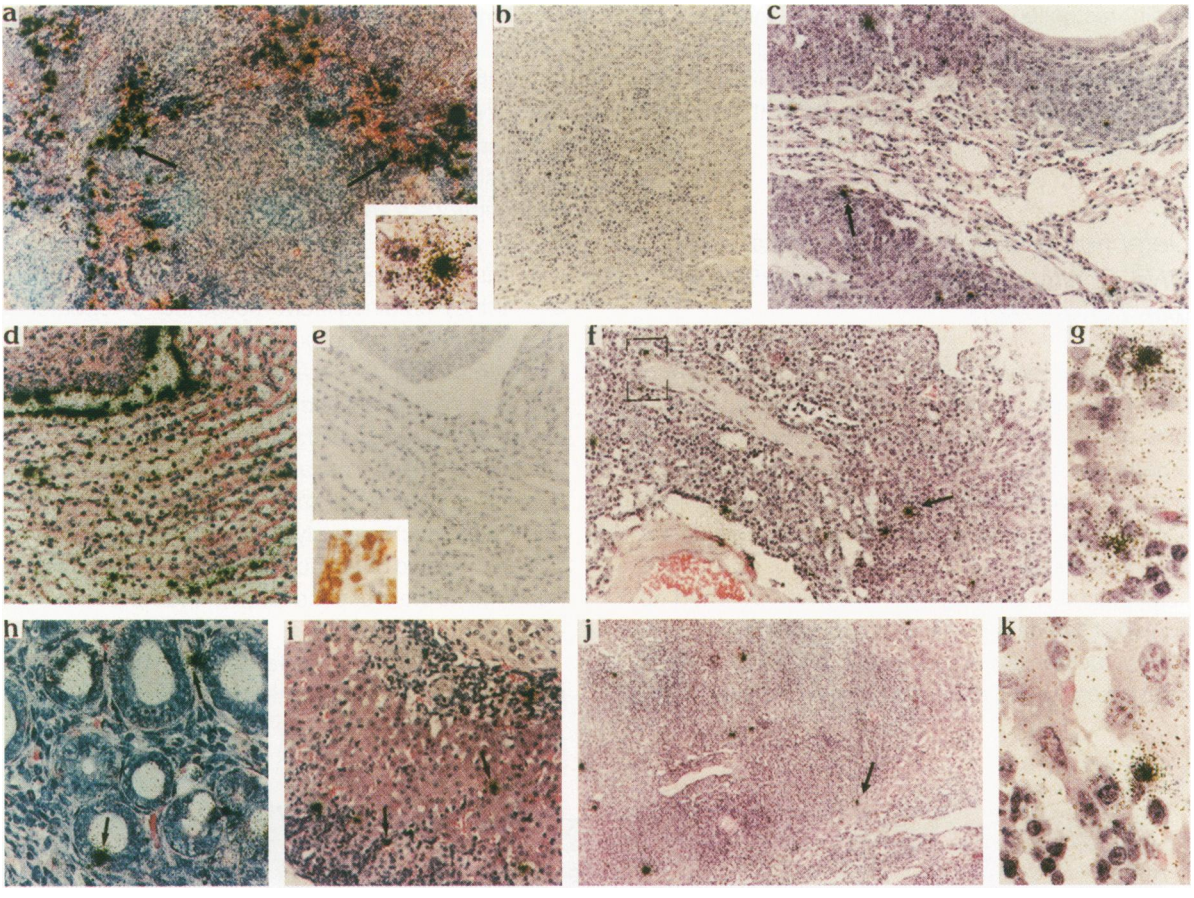

Figure 4. *MHV-68 genome-positive cells associated with lymphomas in various organs as determined by* in situ *hybridization.* **a:** *A large number of lymphoid cells positive for MHV-68 DNA (indicated by arrows) are surrounding lymphomas in the spleen of mouse no. 9 (magnification ×125). Insert shows a magnified view of genome-positive spleen cell (magnification ×1250).* **b:** *Virus antigen was absent from the spleen where viral DNA-positive cells were observed in* (**a**)*, as determined by immunoperoxidase staining of adjacent tissue sections using hyperimmune rabbit polyclonal sera (magnification ×250).* **c:** *Virus genome-positive cells in the lung of a mouse no. 14 with a high grade lymphoma. Massive lymphoid cell accumulations are seen in peribronchiolar and perivascular areas (indicated by an arrow) (magnification ×250).* **d:** *Virus genome-positive cells are seen in the lining of the kidney hilus both on the tubular and lymphoma side of mouse no. 9. Positive cells are also seen within the tubular lumina (magnification ×250).* **e:** *Adjacent section from* (**d**) *stained by immunoperoxidase method for the presence of viral antigen. No antigen-positive cells were detected (magnification ×250). Insert shows a positive control section from an infected lung at 5 days postinfection (magnification ×500).* **f:** *Kidney of mouse no. 22 shows virus genome-positive cells (indicated by an arrow) associated with lymphoma. Note the kidney parenchyma has been largely replaced by abnormal lymphoid tissue (magnification ×250).* **g:** *A magnified view of virus genome-positive cells from* (**f**) *(magnification ×1250).* **h:** *Virus genome-positive cells in the endometrium of mouse no. 22 that developed high grade lymphoma (magnification ×250).* **i:** *Adrenal cortex with virus genome-positive cells (indicated by arrow) associated with lymphocyte infiltrations in mouse no. 22 (magnification ×250).* **j:** *Liver from mouse no. 22 showing virus genome-positive lymphoid cells within a lymphoma (magnification ×125).* **k:** *A magnified view of virus genome-positive lymphoid cells (indicated by an arrow in* j*) among genome-negative hepatocytes (magnification ×1250).*

mas in spleen, mesenteric lymph node, liver, lung, and kidney. Occasional positive cells of lymphoid cell morphology could also be seen in the tissue parenchyma, suggesting perhaps the mode of spread. In the spleen, positive cells were seen primarily in marginal zones or as scattered positive cells throughout the tissue (Figure 4, a). In addition, scattered positive cells were mainly associated with lymphomas observed in liver, kidney, adrenal gland, and endometrium (Figure 4, h, i, and j).

In the kidney, some positive cells were also detected within capillaries and tubular lumen or in the wall (Figure 4, d). Positive cells could be detected in peribronchiolar or perivascular masses of lymphomas in the lungs of mice that developed high grade lymphomas (Figure 4, c). Animals that developed a mild LPD also showed positive cells but these were fewer in number compared with mice with high grade lymphomas.

Again, negative immunoperoxidase staining for virus antigens in adjacent tissue sections using rabbit polyclonal sera strongly suggested that the *in situ*-positive cells are latently infected. None of the animals that developed abnormalities such as adenocarcinomas or atrial thrombosis showed either viral DNA or viral antigens in these affected organs.

Discussion

In a large study of mice chronically infected with MHV-68, LPD was observed in 9% ranging from mild to high grade lymphomas. In all cases virus genome-positive cells were detected either in the lymphoma or associated with the periphery, in some cases appearing in very high numbers. The induction of lymphoid hyperplasia and lymphoid cell infiltration of the parenchyma of organs such as the liver and kidney in MHV-68-infected mice are also features observed in other gammaherpesvirus infections.[3,14]

Why this disease process occurs in mice aged 9 months to 3 years is unclear. One obvious possibility is that such animals may be more prone to immunosuppression than younger animals thus leading to a breakdown in T cell control of latently infected B cells. Certainly treatment of infected animals with CsA to interfere with T cell function produced an increase in the number of animals with lymphomas, arguing for a role for T cells in controlling the emergence of tumors in MHV-68-infected mice. This explanation is in agreement in the events observed in EBV-driven LPD after immunosuppression of virus-positive individuals.[15,16] In such cases the use of immunosuppressive therapy resulted in a lymphoma incidence well above that in the control population. In patients with posttransplant lymphoproliferative disease (PTLPD) the histological appearance varied from polymorphic (composed of a mixture of cell types) to monomorphic proliferations composed of large cells. The majority of these were B lymphocytes, representing polyclonal B cell hyperplasia or clonal B cell neoplasia or lymphoma.[17,18] In MHV-68-infected mice a major site of virus latency is the B lymphocyte and *in vitro* these cells transform spontaneously to generate B cell lines (unpublished observations). In all cases of high grade lymphoma studied thus far, light chain restriction was seen indicating a clonal origin of these B cells. The lymphomas were also composed of CD3-positive T cells, suggesting that these might be responding to virus-infected cells.

The heterogeneous scattered distribution of MHV-68 DNA-positive cells in these lymphomas/lymphoid hyperplasias is similar to the infectious mononucleosis-like pattern described by Borisch-Chappuis et al.[19] for EBV-positive cells in patients with PTLPD. In some cases of high grade lymphomas, such as the spleen of mouse no. 9, a huge number of genome-positive cells were located in the marginal zone and others in the kidney and liver. Such infected cells are not a characteristic feature of lymphomas in EBV-infected patients and may reflect some differences between MHV-68 and EBV. Despite the strong signal over individual infected cells, there was no evidence of lytic viral antigens in adjacent sections of lymphomas, indicating that these lymphoid cells carry multiple copies of latent MHV-68 genomes. A similar picture emerges in PTLPD where the pattern of viral antigen expression is more like that of EBV-transformed cells that lack lytic antigens.[1,2,20]

The failure to detect viral DNA in all cells of a particular lymphoma may be related to various factors. One possibility is that low DNA copy numbers are not detected by our *in situ* hybridization procedure. This proved to be the case for a number of EBV-associated lymphomas that were negative when probed for DNA but positive for the viral transcripts EBERS.[21–23] We have still to identify genes and gene products associated with latency that might allow us to identify virus-positive lymphomas. Regardless of this, the restriction of *in situ*-positive cells primarily to the areas of lymphomas in nonlymphoid tissues of infected mice strongly suggests an association between this virus and the pathogenesis of LPD.

In conclusion, the association of MHV-68 in LPD of mice further highlight the molecular and pathogenic similarities to EBV and therefore identifies this virus as a valuable model for the study of human disease caused by EBV.

Acknowledgments

We thank Drs. S. Wharton and S. Efstathiou for helpful discussions.

References

1. Young L, Alfieri C, Hennessy K, Evans H, O'Hara C, Anderson KC, Ritz J, Shapiro RS, Rickinson A, Kieff E, Cohen JI: Patients with EBV lymphoproliferative disease. N Engl J Med 1989, 321:1080–1085
2. Thomas JA, Hotchin NA, Allday MJ, Amlot P, Rose M, Yacoub M, Crawford DH: Immunohistology of Epstein-Barr virus associated antigens in B cell disorders from immunocompromised individuals. Transplantation 1990, 49:944–953
3. Fleckenstein B, Desrosiers RC: Herpesvirus saimiri and herpesvirus ateles. In The Herpesviruses, vol I. Edited by B Roizman. New York, Plenum Press, 1982, pp 253–321
4. Shope T, Dechairo D, Miller G: Malignant lymphoma in cotton top marmosets after inoculation with Epstein-Barr virus. Proc Natl Acad Sci USA 1973, 70:2487–2491

5. Young LS, Finerty S, Brooks L, Scullion F, Rickinson AB, Morgan AJ: Epstein-Barr virus gene expression in malignant lymphomas induced by experimental virus infection of cotton top tamarins. J Virol 1989, 63:1967–1974
6. Rowe M, Young LS, Crocker J, Stokes H, Henderson S, Rickinson AB: Epstein-Barr virus (EBV)-associated lymphoproliferative disease in the SCID mouse model: implications for the pathogenesis of EBV-positive lymphomas in man. J Exp Med 1991, 173:147–158
7. Cannon MJ, Pisa P, Fox RI, Cooper NR: Epstein-Barr virus induces aggressive lymphoproliferative disorders of human B cell origin in SCID/hu chimeric mice. J Clin Invest 1990, 85:1333–1337
8. Blaskovic D, Steneskova M, Svobodova J, Mistrikova J: Isolation of five strains of herpesviruses from two species of free living rodents. Acta Virol 1980, 24:468
9. Efstathiou S, Ho YM, Hall S, Styles CJ, Scott SD, Gompels UA: Murine herpesvirus 68 is genetically related to the gamma herpes viruses Epstein-Barr virus and herpesvirus saimiri. J Gen Virol 1990b, 71:1365–1372
10. Sunil-Chandra NP, Efstathiou S, Arno J, Nash AA: Virological and pathological features of mice infected with murine gammaherpesvirus 68. J Gen Virol 1992a, 73: 2347–2356
11. Sunil-Chandra NP, Efstathiou S, Nash AA: Murine gammaherpesvirus-68 establishes a latent infection in mouse B lymphocytes in vivo: J Gen Virol 1992b, 73: 3275–3279
12. Sunil-Chandra NP, Efstathiou S, Nash AA: Interactions of murine gammaherpesvirus 68 with B and T cell lines. Virology 1993, 193:825–833
13. Efstathiou S, Ho YM, Minson AC: Cloning and molecular characterisation of the murine herpesvirus 68 genome. J Gen Virol 1990a, 71:1355–1364
14. Roizman B: The family herpesviridae general description, taxonomy, and classification. In The Herpesviruses, vol 1. Edited by B Roizman. New York, Plenum Press, 1982, pp 1–23
15. Randhawa PS, Markin RS, Starzl TE, Demetris AJ: Epstein-Barr virus associated syndromes in immunosuppressed liver transplant recipients: clinical profile and recognition on routine allograft biopsy. Am J Surg Pathol 1990, 14:538–547
16. Hanto DW, Frizzera G, Purtilo DT, Sakamoto K, Sullivan JL, Saemundsen AK, Klein G, Simmons RL, Najarian JS: Clinical spectrum of lymphoproliferative disorders in renal transplant recipients and evidence for the role of Epstein-Barr virus. Cancer Res 1981, 41: 4253–4261
17. Frizzera G, Hanto DW, Gajl-Peczalska KJ, Rosai J, McKenna RW, Sibley RK, Holahan KP, Lindquist IL: Polymorphic diffuse B-cell hyperplasia and lymphomas in renal transplant recipients. Cancer Res 1981, 41:4262–4279
18. Nalesnic MA: Lymphoproliferative disease in organ transplant recipients. Springer Semin Immunopathol 1991, 13:199–216
19. Borish-Chappuis B, Nezelof C, Muller-Hermelink HK: Different Epstein-Barr virus expression in lymphomas from immunocompromised and immunocompetent patients. Am J Pathol 1990, 136:751–758
20. Rickinson AB, Gregory CD, Murray RJ, Ulaeto DO, Rowe M: Cell mediated immunity to Epstein-Barr virus and the pathogenesis of virus associated B cell lymphomas. In Immune Responses, Virus Infections and Disease, vol. 27. Edited by NJ Dimmock, PD Minor, IRL Press, Eynsham, Oxford, UK, 1989, pp 59–83
21. Howe JG, Steitz JA: Localization of Epstein-Barr virus-encoded small RNAs by in situ hybridisation. Proc Natl Acad Sci USA 1986, 83:9006–9010
22. Weiss LM, Mohaved LA: In situ demonstration of Epstein-Barr viral genomes in viral associated B cell lymphoproliferations. Am J Pathol 1989, 134:651–659
23. Deacon EM, Pallesen G, Neidobitec G, Crocker J, Brooks L, Rickinson AB, Young LS: Epstein-Barr virus a Hodgkin's disease: transcriptional analysis of virus latency in the malignant cells. J Exp Med 1993, 177: 339–349